ADVANCES IN ATMOSPHERIC SCIENCES, VOL. 29, NO. 2, 2012, 333–343

The Potential Impacts of Warmer-Continent-Related Lower-Layer Equatorial Westerly Wind on Tropical Cyclone Initiation

YUAN Zhuojian*[1] (袁卓建), QIAN Yu-Kun[1,2] (钱钰坤),
QI Jindian[1] (戚锦典), and WU Junjie[3] (吴俊杰)

[1] *Center for Monsoon and Environmental Research/Department of Atmospheric Science, Sun Yat-sen University, Guangzhou* 510275

[2] *State Key Laboratory of Tropical Oceanography, South China Sea Institute of Oceanology, Chinese Academy of Sciences, Guangzhou* 510301

[3] *Civil Aviation Flight University of China, Guanghan* 618307

(Received 28 June 2011; revised 7 September 2011)

ABSTRACT

Global climate models predict that the increasing Amazonian-deforestation rates cause rising temperatures (increases of 1.8°C to 8°C under different conditions) and Amazonian drying over the 21st century. Observations in the 20th century also show that over the warmer continent and the nearby western South Atlantic Ocean, the lower-layer equatorial westerly wind (LLEWW) strengthens with the initiation of tropical cyclones (TCs). The warmer-continent-related LLEWW can result from the Coriolis-force-induced deflection of the cross-equatorial flow (similar to the well-known heat-island effect on sea breeze) driven by the enhanced land-sea contrast between the warmer urbanized continents and relatively cold oceans. This study focuses on the processes relating the warmer-continent-related LLEWW to the TC initiation and demonstrates that the LLEWW embedded in trade easterlies can directly initiate TCs by creating cyclonic wind shears and forming the intertropical convergence zone. In addition to this direct effect, the LLEWW combined with the rotating Earth can boost additional updraft vapor over the high sea-surface temperature region (factor 1), facilitating a surface-to-midtroposphere moist layer (factor 2) and convective instability (factor 3) followed by diabatic processes. According to previous studies, the diabatic heating in a finite equatorial region also activates TCs (factor 4) on each side of the Equator with weak vertical shear (factor 5). Factors 1–5 are favorable conditions for the initiation of severe TCs. Statistical analyses show that the earliest signal of sustained LLEWW not only leads the earliest signal of sustained tropical depression by >3 days but also explains a higher percentage of total variance.

Key words: tropical cyclone, human activities, climate change, global warming

Citation: Yuan, Z. J., Y.-K. Qian, J. D. Qi, and J. J. Wu, 2012: The potential impacts of warmer-continent-related lower-layer equatorial westerly wind on tropical cyclone initiation. *Adv. Atmos. Sci.*, **29**(2), 333–343, doi: 10.1007/s00376-011-1100-x.

1. Introduction

Numerous studies show that removing Amazonian forests could affect local and global climates in many ways (e.g., Shukla et al., 1990; Nobre et al., 1991; Betts et al., 2004; Morton et al., 2006; Christensen et al., 2007; Costa et al., 2007; Sampaio et al., 2007; Malhi et al., 2008; Nobre et al., 2009). Based on the fact that "from 1988 to 2006, deforestation rates in Brazilian Amazonia averaged 18,100 km^2 yr^{-1}, recently reaching 27,400 km^2 yr^{-1} in 2004" (Malhi et al., 2008, p. 169), global climate models (GCMs) predict warmer and drier climates in the Amazon. Specifically, in the 21st century, increases of 1.8°C to 5.1°C could be associated with midrange greenhouse gas emission (e.g., Christensen et al., 2007; Malhi et al., 2008). Up to 8°C warming in the Amazon could be associated with substantial forest dieback on regional biophysical proper-

*Corresponding author: YUAN Zhuojian, qianyk@mail2.sysu.edu.cn

ties (Betts et al., 2004; Malhi et al., 2008).

Consistently, increasing temperature, averaged over Brazilian Amazonia, was observed in the 20th century (Fig. 1a) with the increase of deforested area. Deforested area increased from about 130 000 km^2 in 1975 to ∼420 000 km^2 in 1991 (Nobre et al., 1991) and ∼560 000 km^2 around 2006 in Brazilian Amazonia alone (Morton et al., 2006; Costa et al., 2007; Sampaio et al., 2007). To show how observed wind fields respond to the warmer continent, Fig. 1b displays the difference in the decadal-mean 850-hPa wind fields between 1997–2006 and 1957–1966 based on the reanalysis data for months of January. In Fig. 1b the lower-layer equatorial westerly wind (LLEWW) appears over the Amazon and the nearby western South Atlantic Ocean (WSAO) together with the activation of tropical cyclones (TCs). Because the deforested area increases with time, the stronger LLEWW over the WSAO can be obtained by subtracting the earlier decadal-mean 850-hPa wind (from 1948 to 1957) from the later decadal-mean 850-hPa wind (from 2001 to 2010; Fig. 1c). Figure 1 suggests that there exist the potential impacts of warmer-continent-induced LLEWW on the TC initiation. It is worth mentioning that 1948 is the earliest year with reanalysis data available. According to Espenshade and Morrison (1986, p23), deforested and urbanized areas increase not only in South America but also across other continents. If the LLEWW and TCs shown in Fig. 1 are, as expected, mainly associated with deforestation and urbanization, then the hurricane-free [referring to the absence of severe TCs (STCs)] climate might be changed in the tropics of South America and the WSAO. One of the signals carried by such a change would be the higher frequency of TC initiation in the tropics around the world if continents warm to a certain extent (Zhang et al., 2010).

The 1948–1978 data-reanalysis does not benefit much from the satellite observations (besides the relatively old techniques used in the old-time measurements); the uncertainty in Fig. 1 is unavoidable. However, the possible processes connecting the deforestation and urbanization to climate changes as suggested by Fig. 1 are of utmost interest. Thus, further observational and statistical analyses were performed to investigate the possibility of mankind-induced climate changes and to justify study of TC initiation by the warmer-continent-related LLEWW with better reanalysis data and common knowledge. Common knowledge is mainly applied to the discussions of the di-

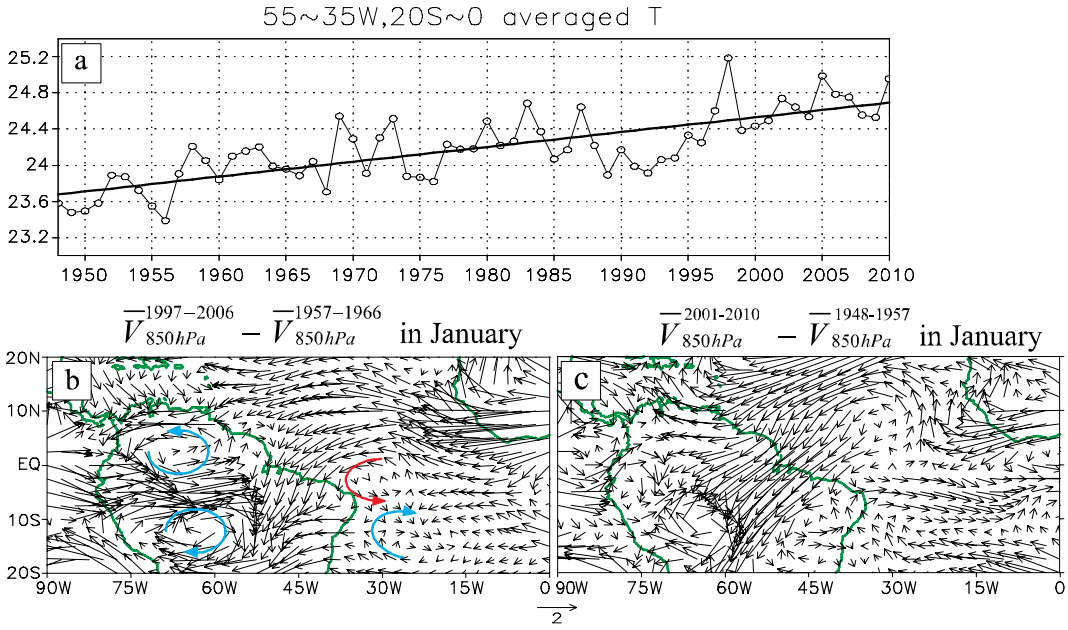

Fig. 1. Based on the NCEP-NCAR reanalysis data, (a) shows the annual mean temperature (open circle) averaged over the region of (0°–20°S, 55°–35°W) and its linear trend (solid line) in the time period 1948–2010; (b) shows the difference between the 1997–2006 decadal-mean 850-hPa wind and the 1957–1966 decadal-mean 850-hPa wind in January. The red curve indicates the cross-equatorial flow deflected by the Coriolis force to form the LLEWW. The blue curves indicate tropical cyclones; (c) shows the difference between the 2001–2010 decadal-mean 850-hPa wind and the 1948–1957 decadal-mean 850-hPa wind in January.

rect (section 3) and indirect (section 4) impacts of the warmer-continent-induced LLEWW on TC initiation. In section 4, traditional TC initial conditions [the surface-to-midtroposphere moist layer over a high sea-surface temperature (SST) region, convective instability characterized by a warmer-and-moist layer located below a cold-and-dry layer, TCs and weak vertical shear of horizontal wind] emphasized by previous studies (e.g., Charney and Eliassen, 1964; Ooyama, 1969; Gray, 1979; Anthes, 1982, p49) are related to the warmer-continent-induced LLEWW. Recent-year records and reanalysis data with higher quality due to advanced techniques (e.g., satellites, see section 2 for methods and data) were applied to the observational and statistical analyses (sections 5 and 6) to extract the climatological evidence for the key point in the discussions. Summary and discussion are given in section 7.

2. Methodology and data

To assess more significant signals of climate changes that might be attributed to the deforestation and urbanization, we sought reanalysis data for all years for which it was available. As mentioned in introduction, no reanalysis data are available prior to 1948. Thus, the 1948–2010 reanalysis data ($2.5^\circ \times 2.5^\circ$) provided by the National Center for Environmental Prediction-National Center for Atmospheric Research (NCEP-NCAR) (Kalnay et al., 1996; Kistler et al., 2001) were used to plot Fig. 1. To determine the linkage of the warmer-continent-related LLEWW and the TC initiation suggested by Fig. 1, further observational and statistical analyses were performed based on higher-resolution horizontal reanalysis data. These higher-quality data included the daily, long-time mean and anomalous (from the mean) zonal wind, geopotential and SST data ($1.5^\circ \times 1.5^\circ$) derived from the European Centre for Medium-Range Weather Forecasts (ECMWF) Reanalysis Archive Interim (ERA-Interim) dataset. Because the daily, long-time mean and anomalous (from the mean) outgoing long-wave radiation (OLR) data were not available at the ECMWF, the OLR data ($2.5^\circ \times 2.5^\circ$) were acquired from the National Oceanic and Atmospheric Administration (NOAA). The composite technique and empirical orthogonal function (EOF) analysis were used to extract the leading signal for the TC initiation carried by the LLEWW before the presence of the initial genesis points of TCs detected by the Joint Typhoon Warning Center (JTWC), National Hurricane Center (NHC), and Japan Meteorological Agency (JMA) for STCs (e.g., hurricanes or typhoons).

The location of the genesis point for the first STC of each year was determined according to the "best track" data at 0000, 0600, 1200, and 1800 UTC from the JTWC, NHC, and JMA. The accuracy of STC records has been improved in recent years due to advanced techniques used in satellites (Chan, 2006; Klotzbach, 2006). Therefore, records for recent years were used in this study.

3. A direct linkage between the warmer-continent-related LLEWW and TC initiation

According to common knowledge (e.g., Ahrens, 1999, p28), (pure) water absorbs four times the heat energy to raise the same amount of temperature, than soil does in terms of per-unit mass (i.e., there is a much smaller heat-capacity difference between the sea and tropical rainforest than that between the sea and urbanized continent). Therefore, solar radiation warms the land more rapidly than the adjacent water. Consequently, urban zones are responsible for the heat-island effect (e.g., Bornstein, 1968; Arnfield, 2003; Dandou et al., 2005; Basara et al., 2008) followed by the well-known sea breeze in which air blows from the sea toward the land.

Likewise, if continents, especially equatorial sides of continents, become warmer due to urbanization and deforestation (such as Brazilian Amazonia shown by observations and predicted by GCMs), then a fresh cross-equatorial flow (from colder oceans in the winter hemisphere to warmer urbanized continents in the summer hemisphere) could be generated by the enhanced land-sea contrast. On the rotating Earth, this cross-equatorial flow would be deflected by the Coriolis force to form the LLEWW. Accompanying the presence of such an external-force-induced significant LLEWW embedded in trade easterlies is the presence of the intertropical convergence zone (ITCZ), the lower-level cyclonic wind shears, and TCs (Fig. 2). This direct activation of the lower-level cyclonic shears with TCs (Fig. 2b) by the LLEWW is accomplished by reducing the peak value (at the equator) of trade easterlies between the Northern Hemisphere and the Southern Hemisphere subtropical high belts (Fig. 2a).

External forces (rather than internal forces) are the focus of the present study for two reasons: First, the Earth's rotation-induced Coriolis force and the deforestation or urbanization followed by the enhanced land-sea differential heating are all factors external to atmospheric motion. Second, we aimed to avoid the "chicken-and-egg" problem associated with the nonlinear feedback of STCs as internal sources of LLEWW (Gao et al., 1988).

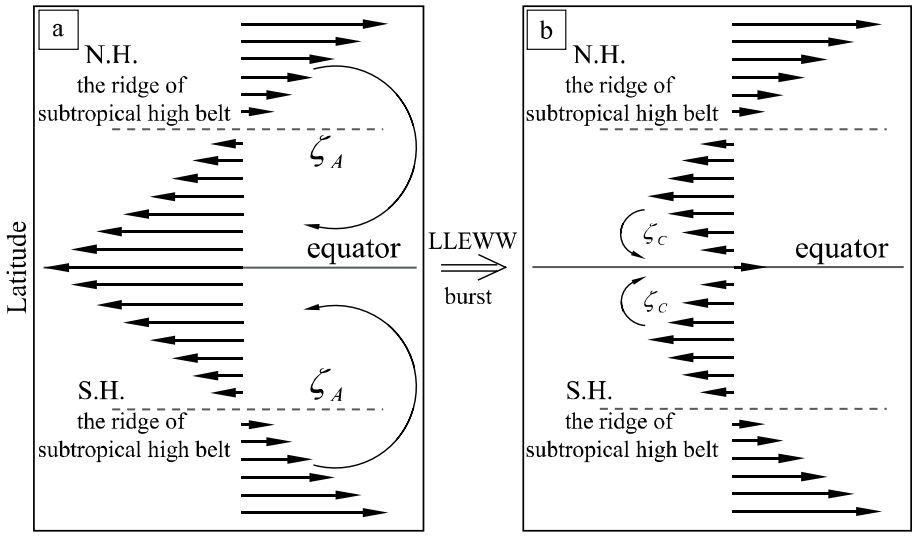

Fig. 2. (a) The zonal flow (thick arrows) distribution with latitude in the balance situation of the zonally homogeneous trade easterlies between the NH and SH subtropical high belts. (b) The one-level cyclonic wind shears on the equatorward side of easterly jets induced by the external-force-induced LLEWW burst. Symbols ζ_A and ζ_C represent anticyclonic and cyclonic vorticities, respectively.

4. An indirect linkage between the warmer-continent-related LLEWW and the TC initiation

As pointed out by Anthes (1982, pp49–51), the traditional TC initial conditions (mentioned in the last paragraph of introduction) are related such that the convective instability depends on the surface-to-midtroposphere moist layer over high SST regions. This high relative humidity in convective clouds makes a significant contribution to diabatic heating (e.g., Anthes, 1982, p51) while the diabatic heating in a finite equatorial region can initiate two TCs on each side of the equator (e.g., Gill, 1980; Hartmann and Hendon, 2007). The LLEWW between these two cyclones creates the weak vertical shear of horizontal wind by reducing the lower-layer trade easterlies beneath the upper-layer westerlies (Figs. 3a and 3b). In this chain

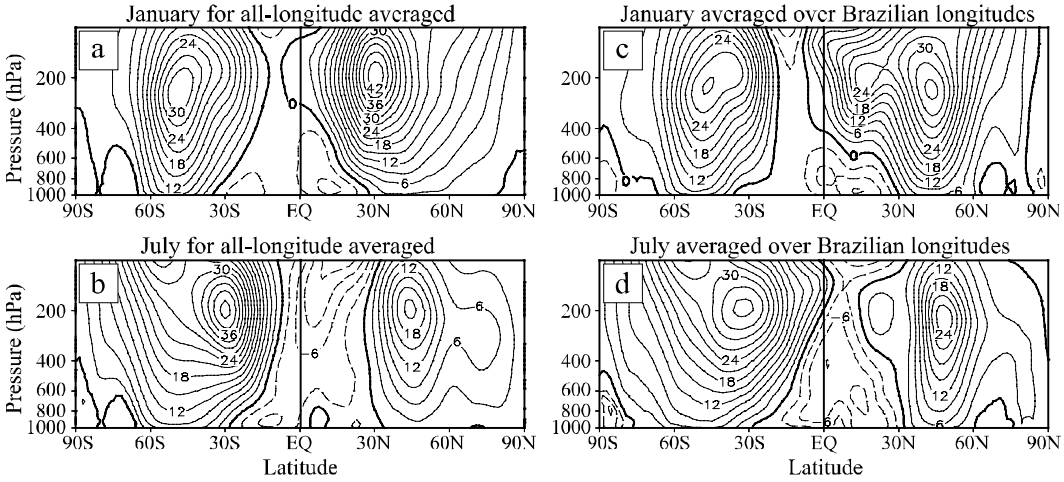

Fig. 3. The vertical-meridional distributions of observed zonal mean easterlies (m s^{-1}, dashed lines) and westerlies (solid lines) for (a) January and (b) July based on the time mean (1989–2008) zonal winds from the ERA-Interim analysis data. The much-straighter, upward, thick solid line in the NH summer indicates the weaker vertical shear due to the presence of LLEWW and the upper-layer equatorial easterlies. Panels (c) and (d) are the same as panels (a) and (b) except for the mean zonal winds over Brazil (70°–30°W).

of processes, the key is the initiation of the rapid upward acceleration of moist air (originally resting at the sea surface) required by the formation of the surface-to-midtroposphere moist layer. Next we demonstrate that even without the presence of trade easterlies in the tropics, the external-force-induced LLEWW could cause an upward acceleration.

At the equator, the relationship between the Earth's relative zonal (u) and vertical (w) velocities is very different from that at the poles. At the poles, the u-plane and the w-plane are perpendicular to each other and the Earth's angular velocity $\boldsymbol{\Omega}$ is parallel to the vertical coordinate $\boldsymbol{k}_{\rm pole} = \boldsymbol{w}_{\rm pole}/|\boldsymbol{w}_{\rm pole}|$ (Fig. 4). However at the equator, the relative velocities (u, w) detected on the rotating Earth are in the same equatorial plane with $\boldsymbol{\Omega}$ perpendicular to $\boldsymbol{k}_{\rm eq} = \boldsymbol{w}_{\rm eq}/|\boldsymbol{w}_{\rm eq}|$ (Fig. 4). Thus, in reality the updraft vapor from the sea surface in the equatorial region can be boosted by the rotating Earth ($\boldsymbol{\Omega} > 0$) working with the external-force-induced LLEWW (u>0, Fig. 4). As illustrated by Fig. 4, if at $t = 0$ an external-force-induced flow (double-line arrows in Fig. 4) is responsible for the Earth-relative velocities (u>0, w=0) at point A, then after the Earth rotates from point A to point B during a short time t=Δt, the external-force-induced flow will account for w>0. Thus, even without the presence of trade easterlies in the tropics, the external-force-induced significant LLEWW could cause an upward acceleration (more significant than the Coriolis-force-induced zonal-wind acceleration in the midlatitudes due to $\cos 0^\circ > \sin 45^\circ$). With the presence of trade easterlies, both the mass-continuity equation and observations justify that the updraft vapor can be strengthened by the ITCZ between the LLEWW and trade easterlies.

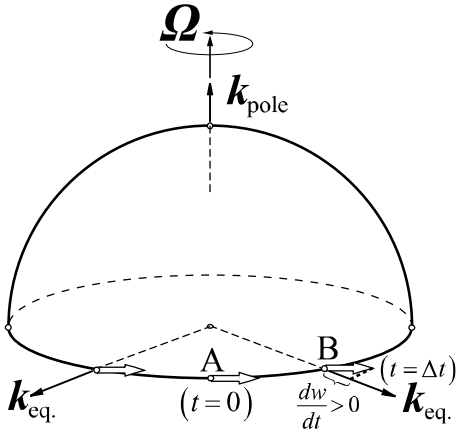

Fig. 4. The upward acceleration at the equator boosted by the external-force-induced LLEWW (double-line arrows) working with the rotating Earth without the presence of trade easterlies.

As reviewed earlier, the updraft vapor (driven by the significant LLEWW) thickens the warm-and-moist layer underneath a cold-and-dry layer, especially in the spring hemisphere with the relatively cold-and-dry troposphere. Consequently, instability and diabatic processes come into play (e.g., Holton, 1979, p50; Yuan and Johnson, 1998; White, 2002, p23; Holton, 2004, p52; Gao et al., 2009; Qian et al., 2011). According to previous studies (e.g., Charney and Eliassen, 1964; Gill, 1980; Hartmann and Hendon, 2007), the diabatic heating in a finite equatorial region can also initiate TCs on each side of the equator. Figure 4 indicates that the external-force-induced LLEWW carries a leading signal for TC initiation.

Because TCs are the internal sources of LLEWW (Gao et al., 1988), if these internal sources are involved in the TC initiation study, then they would easily drag us into the "chicken-and-egg" trap. To reduce the "chicken-and-egg" effect, we concentrated on the initiation of the first STC of each year. Section 6 discusses how to extract from observations the leading signal for TC initiation that is carried by LLEWW.

5. The evidence from climatological information

Figure 4 illustrates a close linkage between the external-force-induced LLEWW and the upward acceleration favorable for the TC initiation. This linkage can also be identified in the climatological information (Fig. 5). Through the comparison between the distribution of the climatological OLR with values $\leqslant$220 W m^{-2} representing the strong upward acceleration according to Gunn et al. (1989) and that of climatological LLEWW, we see that climatological LLEWW centers overlap OLR minimum centers around the Equator (Fig. 5). Figure 5 also shows that although most tropical oceans (including the tropics in the WSAO) experience SST $\geqslant$ 26.5°C, the distribution of initial genesis points of STCs coincides with that of climatological LLEWW better than that of high SST. For example, the seasonal shift of most initial genesis points of STCs coincides quite well with that of climatological LLEWW, especially in the western Pacific equatorial region. The eastern North Pacific tropical region is free from initial genesis points of STCs although the high SST is available in March (with a very weak westerly wind) and April (with a weak westerly wind) until the westerly wind becomes stronger in May. After May (with the observed stronger westerly wind and the presence of initial genesis points of STCs), the region affected by the westerly wind enlarges and the number of initial genesis points of STCs increases substantially,

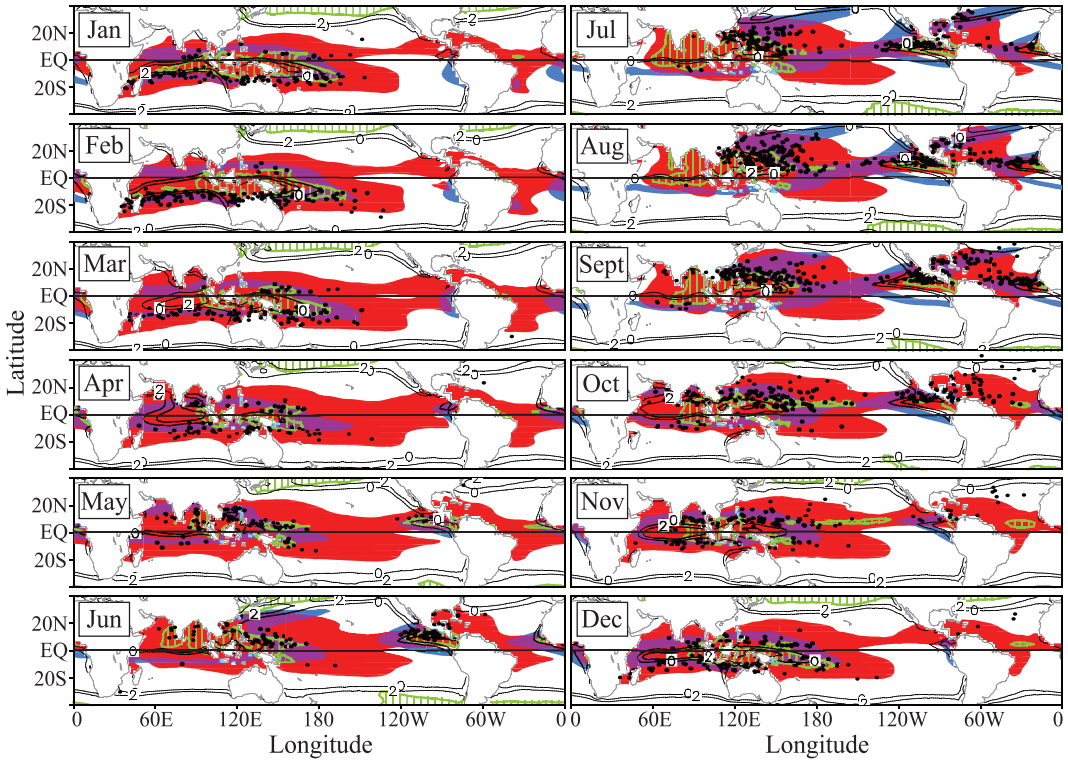

Fig. 5. The distributions of 1989–2008 mean surface westerly winds (thick solid with 0 and 2 m s^{-1} contoured. The zero contour separates the westerly wind region and the easterly wind region in which contours are not shown), the weak vertical shear $|u_{200} - u_{850}|$ ($\leqslant$5 m s^{-1}, blue), high SST ($\geqslant$ 26.5°C, red) and weak OLR ($\leqslant$220 W m^{-2}, green stripes). Purple indicates the areas affected by both SST$\geqslant$26.5°C and weak vertical shear $|u_{200} - u_{850}| \leqslant$5 m s^{-1}. The dots represent the locations of detected initial genesis points of STCs for the 1989–2008 period.

leading to the STC-active season in the eastern North Pacific tropical region. Consistent with Figs. 3a and 3b, the weak vertical shear appears in the regions to the poleward sides of LLEWW (Fig. 5).

We note that in the tropics of the WSAO, the climatological LLEWW (also see Figs. 3c and 3d), OLR minimum centers, STCs together with weak vertical shear are all absent despite the climatological SST $\geqslant$ 26.5°C available throughout the year. In contrast, case studies for Hurricane Catarina (2004) documented as the first hurricane over the WSAO (e.g., Pezza and Simmonds, 2005; McTaggart-Cowan et al., 2006; Pereira Filho, 2010; Vianna et al., 2010) show that SST$<$ 26.5°C is observed in Hurricane Catarina's (2004) spawning area (around 30°S). Consistent with Gray's (1968) argument about the absence of weak vertical shear as a primary reason for the absence of hurricane in the warm tropics of the WSAO, the weak vertical shear associated with a large-scale blocking (e.g., Pezza and Simmonds, 2005; McTaggart-Cowan et al., 2006; Pereira Filho, 2010) and large enthalpy fluxes associated with the surface wind (Vianna et al., 2010) account for Hurricane Catarina (2004). Table 1 and Fig. 12 given by McTaggart-Cowan et al. (2006) show that an extratropical system (as the initial cyclonic vortex for Hurricane Catarina) was detected on 19 March 2004. This extratropical system became a hybrid tropical/extratropical cyclone on 23 March 2004 with weak vertical shear, leading to Hurricane Catarina (2004). The investigation (Fig. 6) in the present study shows that the surface westerly wind had already appeared before the initial extratropical cyclone was detected by satellites.

Figure 5 suggests that the different land-sea contrasts account for the uneven distribution of climatological LLEWW and that of initial genesis points of STCs. This perspective can be justified by two extreme climatological phenomena. One is the most significant LLEWW and the biggest number of initial genesis points of STCs observed in the equatorial region with the most significant land-sea contrast between the largest tropical water (from the Indian Ocean to the western Pacific Ocean) and the largest Eurasian continent (Fig. 5). The other is the absence of climatological LLEWW and TCs over the small tropical area of the WSAO and the small neighboring

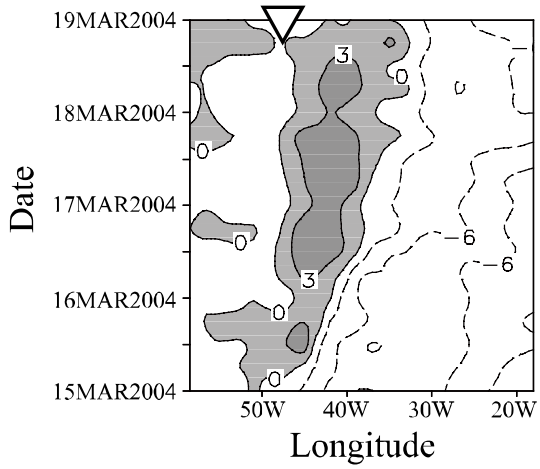

Fig. 6. The time-longitude section of meridionally averaged surface zonal wind (westerly shaded with 3 m s^{-1} interval) obtained from the ERA-Interim data at fixed four-grid points on the equatorward side of the embryonic genesis of the extratropical system (for Hurricane Catarina). The embryonic extratropical system was detected by satellites at (27.0°S, 49.0°W) on 19 March 2004 (see the triangle).

land mostly covered by the tropical rainforest. The evidence presented in this section based on the recent-year observations and the ECMWF reanalysis data verifies (to some extent) the potential impacts of warmer-continent-induced LLEWW on the TC initiation suggested by Fig. 1, which is plotted with the 1948–2010 NCEP-NCAR reanalysis data.

6. Extracting the leading signal for the TC initiation carried by LLEWW from observations

Although it seems impossible to identify the leading signal for the TC initiation carried by LLEWW from the observations in the STC-active season in which the OLR minimum centers do not always overlap the LLEWW centers (not shown), it may be possible to identify the leading signal for the TC initiation carried by LLEWW from the observations in the STC-inactive season (Fig. 7). To extract such a leading signal from observations, we have to rely on statistical methods such as the EOF analysis. The reasons for doing so are that the STC initiation process is a nonlinear and that small-scale processes associated with microphysical phenomena are hard to observe. A sophisticated method is not yet available for accurate numerical solutions of such a process. Additionally, in the STC-active season it is difficult to separate the effect of external-force-induced LLEWW (carrying the leading signal of initial genesis points for STCs) from the effect of STC-induced LLEWW (carrying no such leading signal). Thus, we only focus on the process before the initiation of the first STC of each year.

The first STC of the year is determined based on tropical storm records provided by the JTWC, NHC and JMA. According to Klotzbach (2006) and Chan (2006), the accuracy of the records has improved in recent years due to advanced techniques used in satellites. Thus, the EOF analysis was performed based on

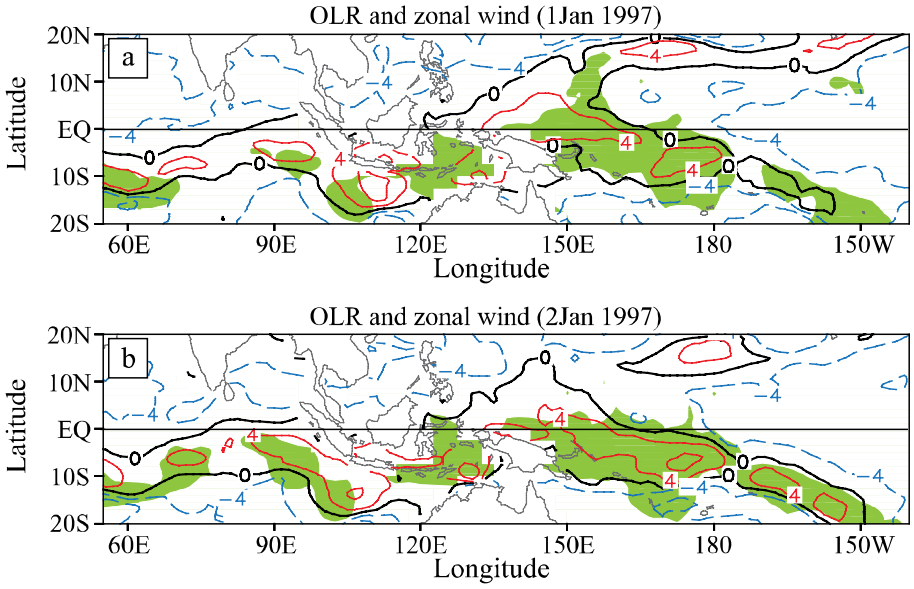

Fig. 7. The distributions of daily surface zonal winds with the interval of 4 m s^{-1} (red solid for westerly and blue dashed for easterly) and daily OLR $\leqslant$ 220 W m^{-2} (green) on (a) 1 January 1997 and (b) 2 January 1997 over the warm tropical ocean.

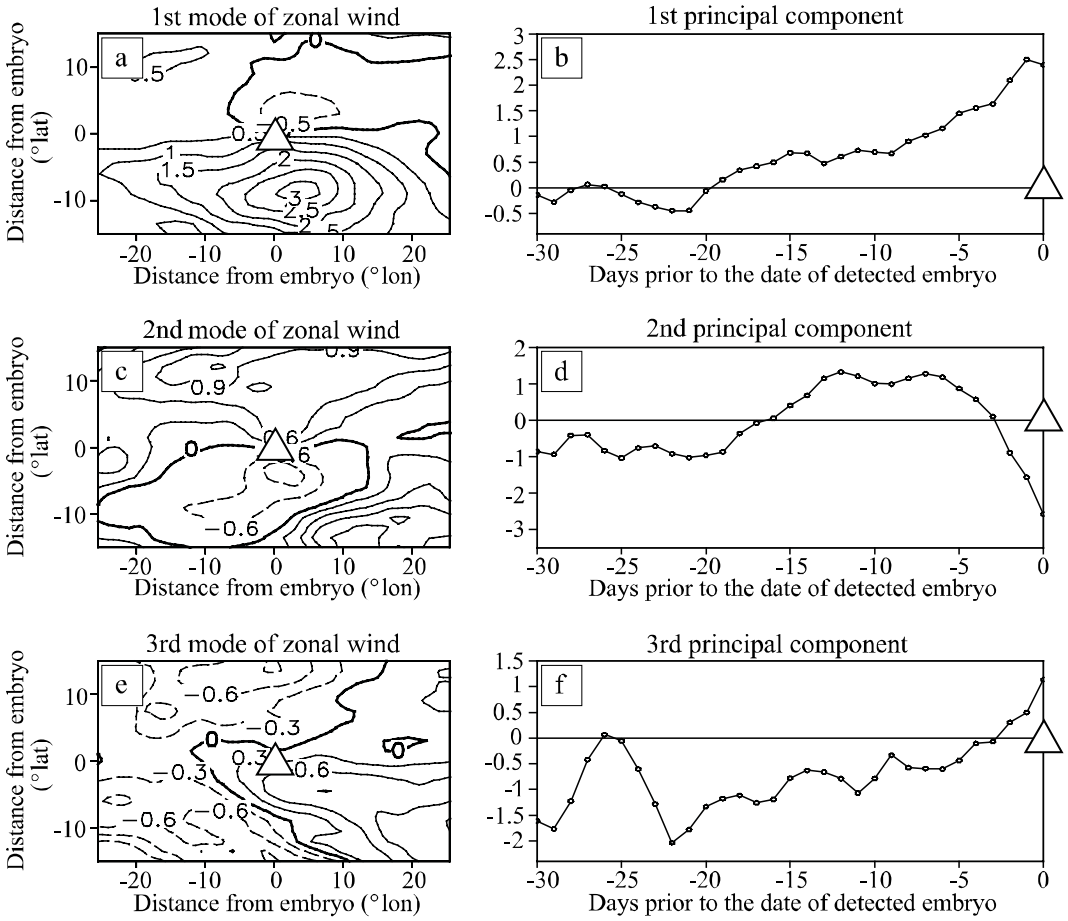

Fig. 8. The EOF-analysis results of 1999–2008 composite 850-hPa zonal wind anomaly departing from the 1989–2008 base period mean based on the ERA-Interim analysis daily data. The composite detected initial genesis point of STC (indicated by the triangle) for the first typhoon of the year is centered at (0, 0). In the left panels, the y-axis (x-axis) is labeled every 10° latitude (longitude) away from the center of the detected initial genesis point of STC. In the right panels, the x-axis is labeled every 5 days prior to the date of detected initial genesis point of STC. The three leading EOF modes explain, respectively 48.1% (a, b), 16.5% (c, d), and 13.0% (e, f) of the total variance.

2000–2009 composite records.

The three leading EOF modes of the composite 850-hPa zonal wind, respectively account for 48.1%, 16.5%, and 13% of the total variance (Fig. 8). The spatial patterns, respectively associated with these three modes (Figs. 8a, 8c and 8e) all show an out-of-phase relationship between the 850-hPa zonal wind to the north and that to the south of the composite center of initial genesis points of STCs. So the signal for the transition from the equatorial easterly wind to the sustained equatorial westerly wind can be identified clearly by the corresponding three time series of the expansion coefficients. This transition happens 20 days and 3 days prior to the presence of the composite initial genesis points of STCs according to the first, second, and third modes, respectively (Figs. 8b, 8d and 8f).

The three leading EOF modes of the composite 850-hPa geopotential, respectively account for 54.5%, 16.8%, and 12.2% of the total variance (Fig. 9). The spatial patterns, respectively associated with these three modes (Figs. 9a, 9c and 9e) all show a homogeneous correlation in the geopotential around the composite center of the initial genesis points of STCs. So the signal for the transition from the high to the sustained low can be identified clearly by the corresponding three time series of the expansion coefficients. This transition happens almost 17 days, 5 days and almost 2 days prior to the presence of the composite initial genesis points of STCs according to the third, second, and first modes, respectively (Figs. 9f, 9d and 9b). The leading signal carried by the LLEWW shown in this section can also be identified in a previous TC activity study (Wu and Chu, 2007). Taking a closer look

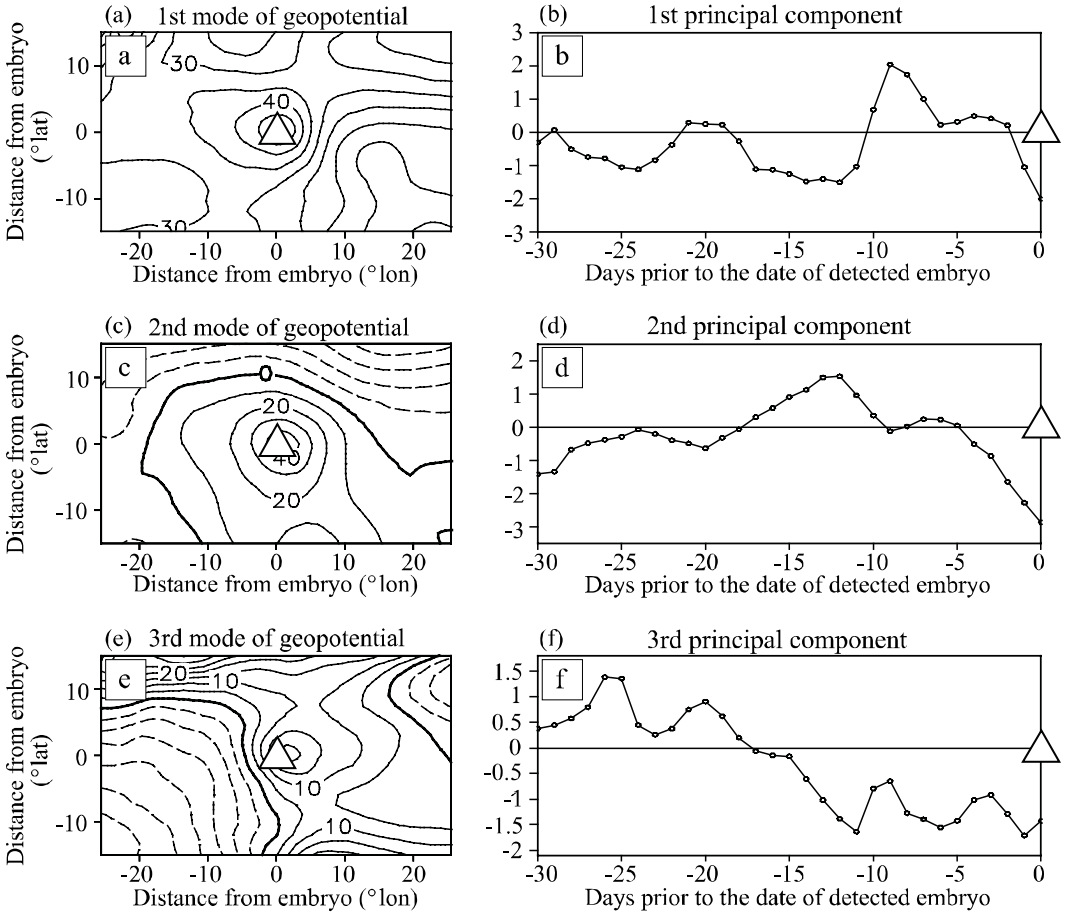

Fig. 9. Same as Fig. 8 except for the geopotential anomaly. The first, second, and third EOF modes account for 54.5%, 16.8%, and 12.2% of the total variance, respectively.

at Fig. 11 given by Wu and Chu (2007), we might say that the westerly wind anomaly appears long before the TC genesis over the eastern North Pacific Ocean.

The above results of EOF analysis also show that the earliest signal of the sustained LLEWW not only leads the earliest signal of the sustained tropical low system by more than 3 days but also becomes more significant in terms of explaining the total variance. These results are consistent with common knowledge. According to common knowledge, when the external-force-induced LLEWW is the cause and the depression is the effect, then the extracted signal of the cause not only leads the extracted signal of the effect but also becomes more significant in terms of explaining the total variance. These "cause-and-effect" characteristics are even more obvious when it takes place in the tropics around the Equator where strong winds can be associated with a weak pressure system (Trenberth et al., 1998). Because a certain time is required for the geopotential (the effect) to respond to the evolution of external-force-induced LLEWW (the cause), during this time, the nonlinear interactions of many processes might weaken the linear relations between the LLEWW EOF modes and the geopotential EOF modes.

7. Summary and discussion

The fate of Amazonian forests and the associated local and global climate changes have received much attention (e.g., Shukla et al., 1990; Nobre et al., 1991; Malhi et al., 2008) due to the fact that "from 1988 to 2006, deforestation rates in Brazilian Amazonia averaged 18,100 km^2 yr^{-1}, recently reaching 27,400 km^2 yr^{-1} in 2004" (Malhi et al., 2008, p169). Based on these deforestation rates, GCMs predict warmer (increases of 1.8°C to 8°C due to different conditions) and drier climates in the Amazon.

These results alert us to the potential activation of more TCs (Zhang et al., 2010) by the continent warming due to worldwide urbanization. It is well known that urbanization leads to the heat-island effect (e.g., Bornstein, 1968; Arnfield, 2003; Dandou et al., 2005; Basara et al., 2008) and the enlarged land-

sea contrast with the stronger sea breeze. The stronger sea breeze induced by the enlarged land-sea contrast could enhance the cross-equatorial flow. On the rotating Earth, the enhanced cross-equatorial flow will be deflected by the Coriolis force to form the LLEWW. The TC initiation by the warmer-continent-related LLEWW could be both direct and indirect. On one hand, the warmer-continent-related LLEWW embedded in trade easterlies could directly initiate TCs and the updraft vapor by creating cyclonic wind shears and forming the ITCZ. On the other hand, the warmer-continent-related LLEWW working with the rotating Earth can boost additional updraft vapor even without the presence of trade easterlies. The updraft vapor then thickens the surface-to-midtroposphere moist layer over a high SST region to build up the convective instability followed by diabatic processes. Gill's model (Gill, 1980) indicates that diabatic heating in a finite equatorial region will also activate TCs on each side of the Equator with weak vertical shear. Therefore, the urbanization-related LLEWW has the potential to initiate TCs in both direct and indirect ways over warm tropical water. With higher-quality data from the ECMWF, JTWC, NHC, and JMA, the results from a EOF analysis indicate that the earliest sustained LLEWW appears at least 3 days prior to the presence of the earliest sustained low pressure system. The corresponding EOF mode of the LLEWW also explains a higher percentage of total variance. The discussions about common knowledge in sections 3 and 4, the further observational and statistical analyses in sections 5 and 6 based on the recent-year observations, and the higher-quality reanalysis data all provide the evidence for the potential initiation of TC attributed to the warmer-continent-induced LLEWW. We emphasize the potential initiation because the urbanization-related LLEWW is only one of LLEWW components. A quantitative estimation for the effect of such a LLEWW component on the TC initiation is hard to conduct without the urbanization-related LLEWW dominating the LLEWW components associated with other external and internal forces. Moreover, the fate of a newly initiated TC characterized by a small-scale perturbation with cyclonic shear can be affected by many factors. For example, the small-scale perturbation might die out before it can be detected. For these reasons, the changes of TC number in the real atmosphere could not tell the story of how the TC initiation is affected by the urbanization-related LLEWW, although Hurricane Catarina (2004) was documented as the first STC over the hurricane-free WSAO.

Acknowledgements. This study was jointly sponsored by the National Key Basic Research Project of China (2009CB421404), the key project of National Natural Science Foundation of China (Grant No. 40730951) and National Natural Science Foundation of China (Grant No. 40575021).

REFERENCES

Ahrens, C. D., 1999: *Meteorology Today: An Introduction to Weather, Climate, and the Environment*. 6th ed., Brooks/Cole Pub Co, 528pp.

Anthes, R. A., 1982: *Tropical Cyclones: Their Evolution, Structure and Effects*. American Meteorological Society, Ephrata, PA, 208pp.

Arnfield, A. J., 2003: Two decades of urban climate research: A review of turbulence, exchanges of energy and water, and the urban heat island. *Int. J. Climatol.*, **23**, 1–26.

Basara, J. B., P. K. Hall Jr., A. J. Schroeder, B. G. Illston, and K. L. Nemunaitis, 2008: Diurnal cycle of the Oklahoma city urban heat island. *J. Geophys. Res.*, **113**, D20109.

Betts, R. A., P. M. Cox, M. Collins, P. P. Harris, C. Huntingford, and C. D. Jones, 2004: The role of ecosystem-atmosphere interactions in simulated Amazonian precipitation decrease and forest dieback under global climate warming. *Theor. Appl. Climatol.*, **78**, 157–175.

Bornstein, R. D., 1968: Observations of the urban heat island effect in New York city. *J. Appl. Meteor.*, **7**, 575–582.

Chan, J. C. L., 2006: Comment on "changes in tropical cyclone number, duration, and intensity in a warming environment". *Science*, **311**, 1713b.

Charney, J. G., and A. Eliassen, 1964: On the growth of the hurricane depression. *J. Atmos. Sci.*, **21**, 68–75.

Christensen, J. H., and Coauthors, 2007: Regional climate projections. *Climate Change, 2007: The Physical Science Basis. Contribution of Working Group I to the Fourth Assessment Report of the Intergovernmental Panel on Climate Change*, Solomon et al., Eds., Cambridge University Press, 847–940.

Costa, M. H., S. N. M. Yanagi, P. J. O. P. Souza, A. Ribeiro, and E. J. P. Rocha, 2007: Climate change in amazonia caused by soybean cropland expansion, as compared to caused by pastureland expansion. *Geophys. Res. Lett.*, **34**, L07706.

Dandou, A., M. Tombrou, E. Akylas, N. Soulakellis, and E. Bossioli, 2005: Development and evaluation of an urban parameterization scheme in the Penn State/NCAR Mesoscale Model (MM5). *J. Geophys. Res.*, **110**, D10102.

Espenshade, E. B., Jr., and J. L. Morrison, 1986: *Goode's World Atlas*. 17th ed., Rand McNally & Company, New York, 367pp.

Gao, S., J. Wang, and Y. Ding, 1988: The triggering effect of near-equatorial cyclones on El Niño. *Adv. Atmos. Sci.*, **5**, 87–96.

Gao, S., F. Zhou, and L. LIu, 2009: Instability of symmetric typhoon circulation and adaptive observation. *Journal of Tropical Meteorology*, **15**, 162–166.

Gill, A. E., 1980: Some simple solutions for heat-induced tropical circulation. *Quart. J. Roy. Meteor. Soc.*, **106**, 447–462.

Gray, W. M., 1968: Global view of the origin of tropical disturbances and storms. *Mon. Wea. Rev.*, **96**, 669–700.

Gray, W. M., 1979: Hurricanes: Their formation, structure, and likely role in the tropical circulation. *Meteorology over the Tropical Oceans*, Shaw, Ed., Royal Meteorological Society, 155–218.

Gunn, B. W., J. L. McBride, G. J. Holland, T. D. Keenan, and N. E. Davidson, 1989: The Australian summer monsoon circulation during AMEX Phase II. *Mon. Wea. Rev.*, **117**, 2554–2574.

Hartmann, D. L., and H. H. Hendon, 2007: Resolving an atmospheric enigma. *Science*, **318**, 1731–1732.

Holton, J. R., 1979: *An Introduction to Dynamic Meteorology*. 2nd ed., Academic Press, New York, 391pp.

Holton, J. R., 2004: *An Introduction to Dynamic Meteorology*. 4th ed., *International Geophysics Series*, Elsevier Academic Press, New York, 535pp.

Kalnay, E., and Coauthors, 1996: The NCEP/NCAR 40-year reanalysis project. *Bull. Amer. Meteor. Soc.*, **77**, 437–471.

Kistler, R., and Coauthors, 2001: The NCEP-NCAR 50-year reanalysis: Monthly means cd-rom and documentation. *Bull. Amer. Meteor. Soc.*, **82**, 247–267.

Klotzbach, P. J., 2006: Trends in global tropical cyclone activity over the past twenty years (1986–2005). *Geophys. Res. Lett.*, **33**, L10805.

Malhi, Y., J. T. Roberts, R. A. Betts, T. J. Killeen, W. Li, and C. A. Nobre, 2008: Climate change, deforestation, and the fate of the Amazon. *Science*, **319**, 169–172.

McTaggart-Cowan, R., L. F. Bosart, C. A. Davis, E. H. Atallah, J. R. Gyakum, and K. A. Emanuel, 2006: Analysis of Hurricane Catarina (2004). *Mon. Wea. Rev.*, **134**, 3029–3053.

Morton, D. C., and Coauthors, 2006: Cropland expansion changes deforestation dynamics in the southern Brazilian Amazon. *Proc. Natl. Acad. Sci. USA*, **103**, 14637–14641.

Nobre, C. A., P. J. Sellers, and J. Shukla, 1991: Amazonian deforestation and regional climate change. *J. Climate*, **4**, 957–988.

Nobre, P., M. Malagutti, D. F. Urbano, R. A. F. de Almeida, and E. Giarolla, 2009: Amazon deforestation and climate change in a coupled model simulation. *J. Climate*, **22**, 5686–5697.

Ooyama, K., 1969: Numerical simulation of the life cycle of tropical cyclones. *J. Atmos. Sci.*, **26**, 3–40.

Pereira Filho, A. J., A. B. Pezza, I. Simmonds, R. S. Lima, and M. Vianna, 2010: New perspectives on the synoptic and mesoscale structure of Hurricane Catarina. *Atmos. Res.*, **95**, 157–171.

Pezza, A. B., and I. Simmonds, 2005: The first South Atlantic hurricane: Unprecedented blocking, low shear and climate change. *Geophys. Res. Lett.*, **32**, L15712.

Qian, Y.-K., C.-X. Liang, Q. Liang, L. Lin, and Z. Yuan, 2011: On the forced tangentially-averaged radial-vertical circulation within vortices. Part II: The transformation of Tropical Storm Haima (2004). *Adv. Atmos. Sci.*, **28**, 1143–1158, doi: 10.1007/s00376-010-0060-x.

Sampaio, G., C. Nobre, M. H. Costa, P. Satyamurty, B. S. Soares-Filho, and M. Cardoso, 2007: Regional climate change over eastern Amazonia caused by pasture and soybean cropland expansion. *Geophys. Res. Lett.*, **34**, L17709.

Shukla, J., C. Nobre, and P. Sellers, 1990: Amazon deforestation and climate change. *Science*, **247**, 1322–1325.

Trenberth, K. E., G. W. Branstator, D. Karoly, A. Kumar, N.-C. Lau, and C. Ropelewski, 1998: Progress during TOGA in understanding and modeling global teleconnections associated with tropical sea surface temperatures. *J. Geophys. Res.*, **103**, 14291–14324.

Vianna, M. L., V. V. Menezes, A. B. Pezza, and I. Simmonds, 2010: Interactions between Hurricane Catarina (2004) and warm core rings in the South Atlantic Ocean. *J. Geophys. Res.*, **115**, C07002.

White, A. A., 2002: A view of the equations of meteorological dynamics and various approximations. *Large-Scale Atmosphere-Ocean Dynamics I: Analytical Methods and Numerical Models*, Norbury and Roulstone, Eds., Cambridge University Press, 1–100.

Wu, P., and P.-S. Chu, 2007: Characteristics of tropical cyclone activity over the eastern North Pacific: The extremely active 1992 and the inactive 1977. *Tellus*, **59A**, 444–454.

Yuan, Z., and D. R. Johnson, 1998: The role of diabatic heating, torques and stabilities in forcing the radial-vertical circulation within cyclones. Part II: Case study of extratropical and tropical cyclones. *Adv. Atmos. Sci.*, **15**, 447–488.

Zhang, Y., H. Wang, J. Sun, and H. Drange, 2010: Changes in the tropical cyclone genesis potential index over the western North Pacific in the SRES A2 scenario. *Adv. Atmos. Sci.*, **27**, 1246–1258, doi: 10.1007/s00376-010-9096-1.